Supporting Information

Hydrophobic Pillared Square Grids for Selective Removal of $CO_2$from Simulated Flue Gas

Sameh K. Elsaidi,[†,⊥] Mona H. Mohamed,[†‡] Todd T. Schaef,[⊥]Amrit Kumar,[§] Matteo Lusi,[§] Tony Pham,[‡] Katherine A. Forrest,[‡] Brian Space,[‡] Wenqian Xu,[¢] Gregory J. Halder,[¢] Jun Liu[⊥,] Michael J. Zaworotko,[*,§] and Praveen K. Thallapally[⊥,*]

[†]Chemistry Department, Faculty Of Science, Alexandria University, P.O.Box 426 Ibrahimia, Alexandria 21321, Egypt

[⊥]Fundamental and Computational Science Directorate, Pacific Northwest National Laboratory, Richland, WA 99352, USA

[‡]Department of Chemistry, University of South Florida, 4202 East Fowler Avenue, CHE205, Tampa, Florida, 33620-5250, USA

[§]Department of Chemical & Environmental Sciences, University of Limerick, Limerick, Republic of Ireland

[¢]X-ray Science Division, Advanced Photon Source, Argonne National Laboratory, Argonne, Illinois, 60439, USA

Methods:

Preparation of $[Co(pz)_2(SiF_6)_2]$, SIFSIX-3-Co:

SIFSIX-3-Co was synthesized by solvothermal reaction of cobalt silicofluoride, $CoSiF_6$ (1 mmol, 0.2 g) with pyrazine, pz,(2 mmol, 0.16 g) in 20 ml methanol at 85 °C. Red crystals were thereby afforded after 3 days thencollected from the Teflon bomb and washed by methanol.

Preparation of $[Ni(pz)_2(SiF_6)_2]$, SIFSIX-3-Ni:

SIFSIX-3-Co was synthesized by solvothermal reaction of nickel silicofluoride, $NiSiF_6$,(1 mmol, 0.20 g) with pyrazine, pz,(2 mmol, 0.16 g) in 20 ml methanol at 85 °C. Blue powder was thereby afforded after 3 days thencollected from the Teflon bomb and washed by methanol.

Sample activation:

The as-synthesized sample of SIFSIX-3-Ni or SIFSIX-3-Co were exchanged with methanolfor 3 days (2 times/day) prior the activation. The resulting solid was filtered and evacuated at 75^{o}C for 15 h under dynamic pressure (<5μm Hg). Due to the strong interaction between CO_2 and the framework which is accompanied by slow CO_2 sorption kinetics, we had increased the equilibrium time during the CO_2 adsorption measurements.

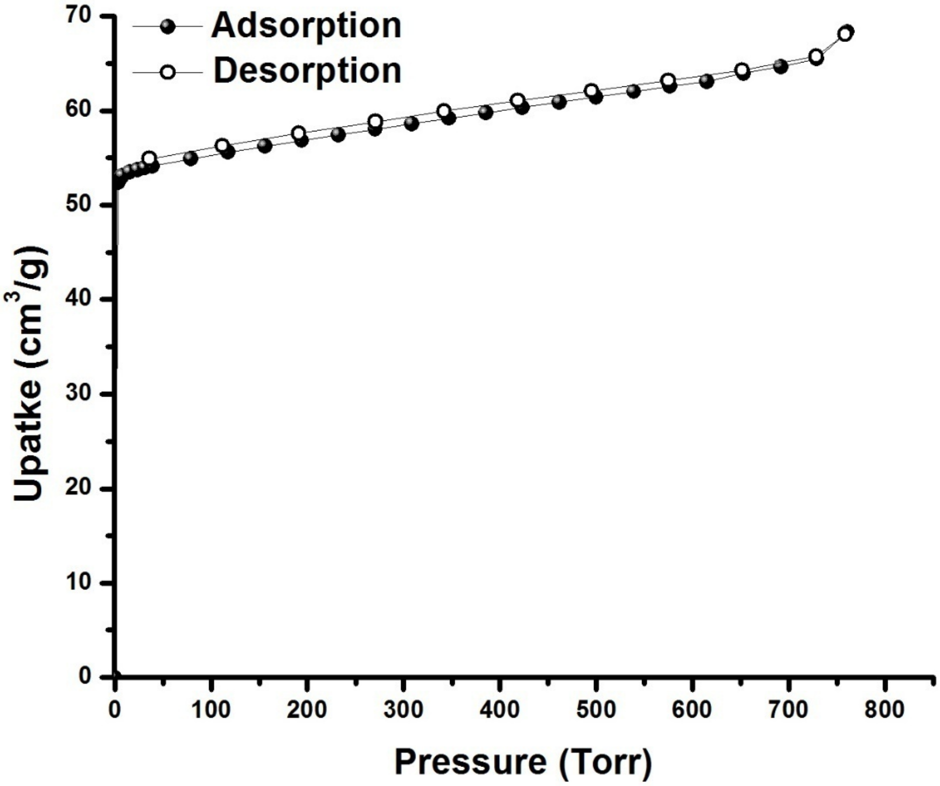

Figure S1: Single component N_2 isotherm collected at 77 K for SIFSIX-3-Co.

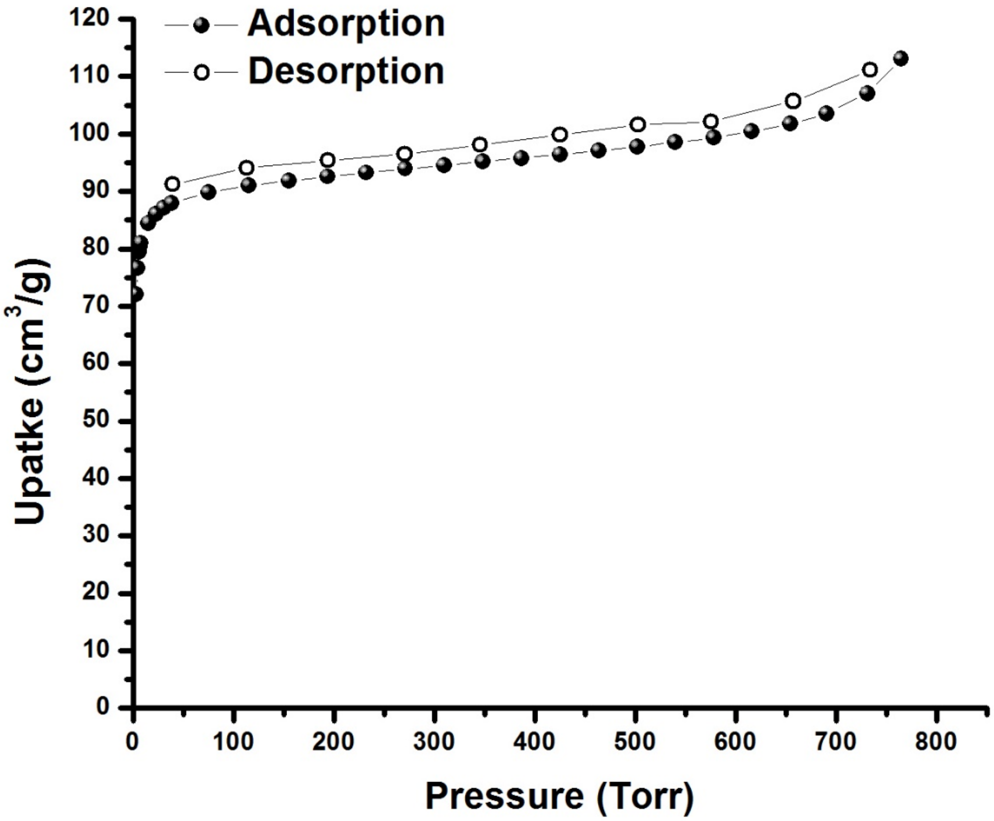

Figure S2: Single component N_2 isotherm collected at 77 K for SIFSIX-3-Ni.

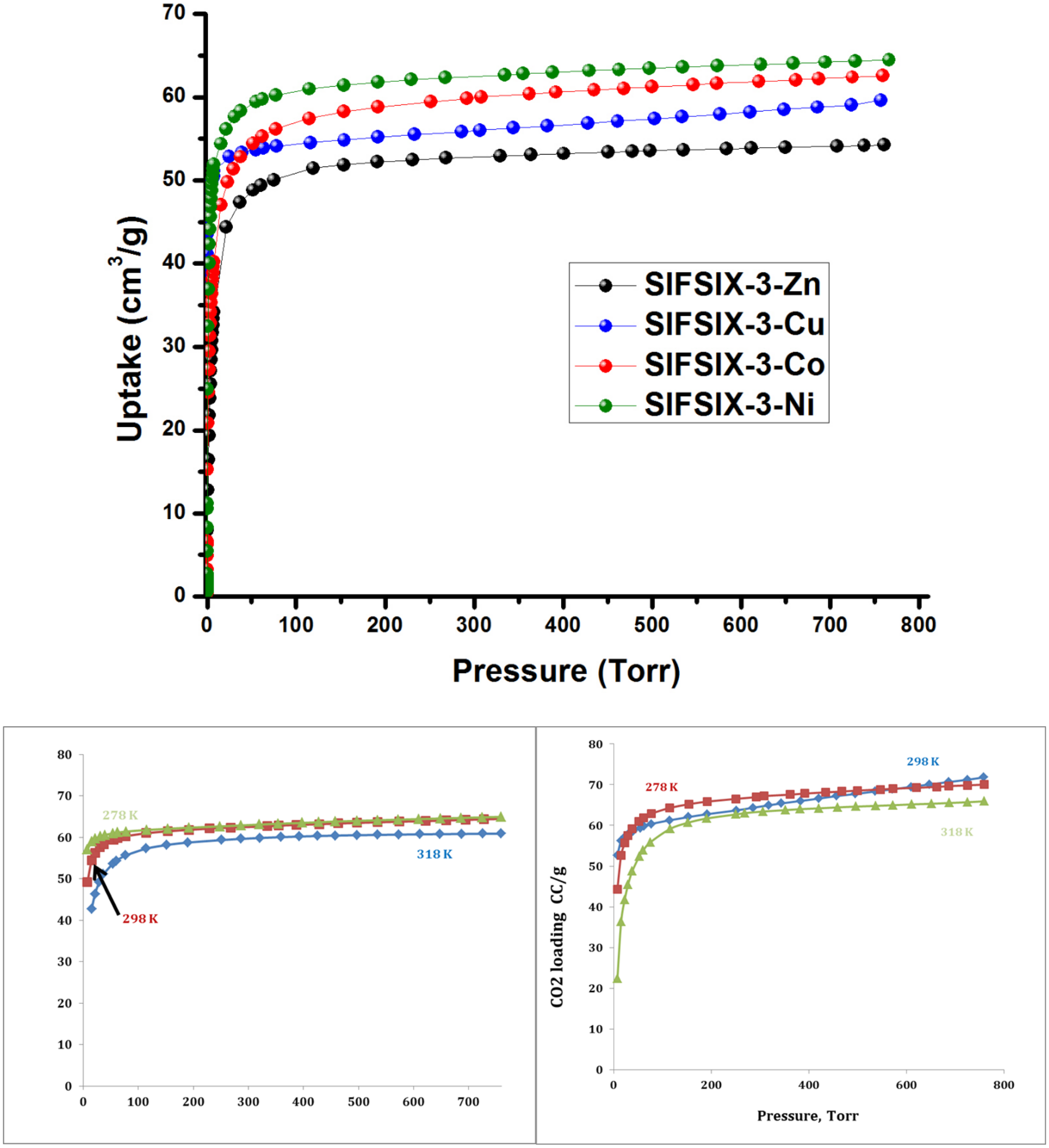

Figure S3: Single component CO_2 adsorption isotherms for SIFSIX-3-Zn, SIFSIX-3-Cu, SIFSIX-3-Co and SIFSIX-3-Ni measured at 298K (top). The bottom figures shows the CO2 loading at different temperatures (SIFSIX-3-Ni, left and SIFSIX-3-Co right).

Isosteric heat of adsorption:

The CO_2isosteric heat of adsorption for SIFSIX-3-Ni and SIFSIX-3-Co were calculated by dual-site Langmuir-Freundlich equation:

$$n = \frac{n_{m1} b_1 P^{\left(\frac{1}{t_1}\right)}}{1 + b_1 P^{\left(\frac{1}{t_1}\right)}} + \frac{n_{m2} b_2 P^{\left(\frac{1}{t_2}\right)}}{1 + b_2 P^{\left(\frac{1}{t_2}\right)}}$$

where

$$b_1 = b_{01} e^{\left(\frac{E_1}{RT}\right)}$$

$$b_2 = b_{02} e^{\left(\frac{E_2}{RT}\right)}$$

In this equation, n is the amount sorbed per mass of sorbent (in mmol g^{-1}), P is the total pressure (in kPa), R is the ideal gas constant, n_{m1}, b_{01}, b_1, E_1, and t_1 are the saturation uptake (in mmol g^{-1}), the pre-exponenetial factor (in kPa^{-1}), the affinity coefficient (in kPa^{-1}) , the activation energy (in kJ mol^{-1}), and the deviation from the ideal homogeneous surface (unitless) for site 1, respectively, and n_{m2}, b_{02}, b_2, E_2, and t_2 are analogous parameters for site 2. The parameters that were obtained from the simultaneous fitting are found in **Table S1**.

Table S1: The fitted parameters for the dual-site Langmuir-Freundlich equation for the single-component isotherms of CO_2 in SIFSIX-3-Ni and SIFSIX-3-Co.

	SIFSIX-3-Ni	**SIFSIX-3-Co**
n_{m1} (mol kg^{-1})	2.80207736	2.49387847
b_{01} (kPa^{-1})	7.31E-04	1.60E-06
t_1	6.67421401	1.19303034
E_1	12.47243015	34.0390432
n_{m2} (mol kg^{-1})	2.35374705	0.90966544
b_{02} (kPa^{-1})	5.00E-09	3.17E-04
t_2	0.95893874	11.3216644

E_2	50.9306980	17.0898993

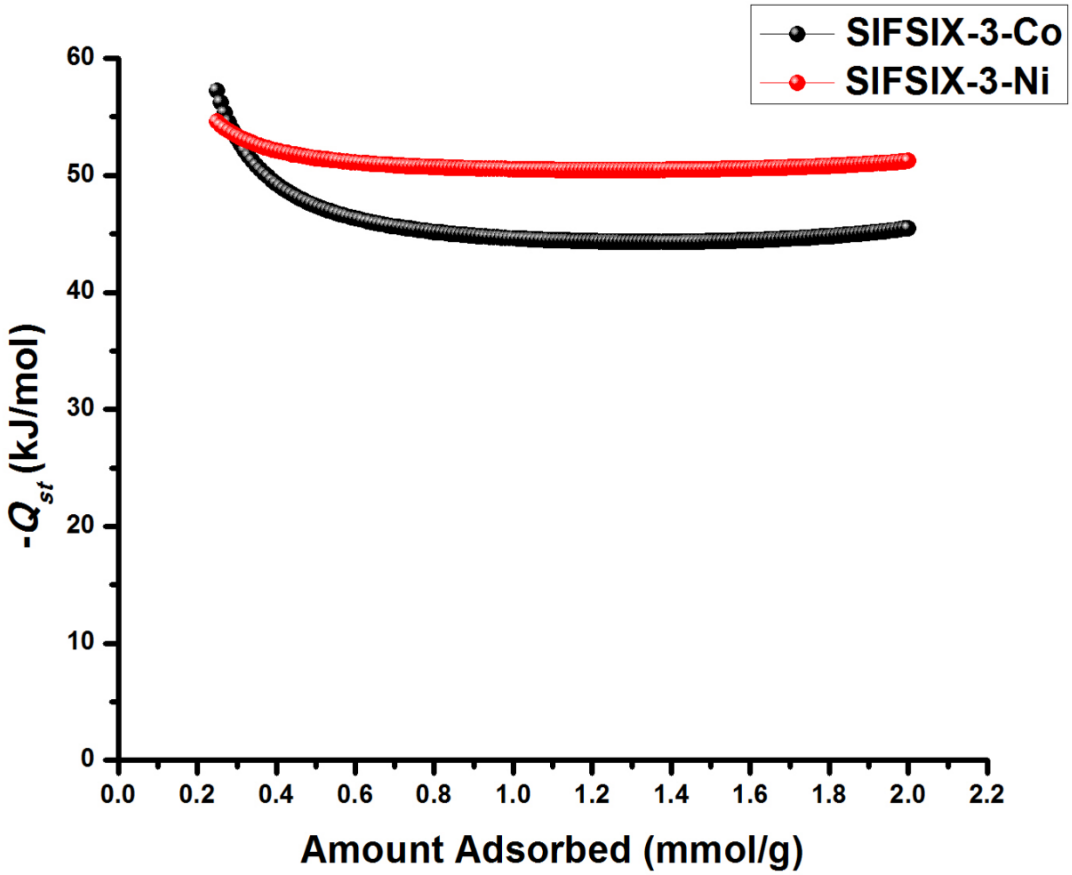

Figure S4: CO_2isosteric heats of adsorption for SIFSIX-3-Ni and SIFSIX-3-Co.

Column breakthrough experiments for CO_2/N_2 gas mixture

Column breakthrough measurements were conducted by packing 0.15-0.5 g of SIFSIX-3-Zn, SIFSIX-3-Cu, SIFSIX-3-Ni or SIFSIX-3-Co sample in a 6.35-cm long and 0.5-cm diameter column. The sample was activated at the activation temperature. The column was cooled to room temperature and the pure He gas was initially flowed to a Stanford Research residual gas analyzer (RGA) for first three minutes, after which the flow of He is stopped and flow of the 15:85 CO_2/N_2gas mixture isintroduced to the fixed bed column containing the MOM sample with flow rate of 1 ml/min and total pressure of 1 bar at room temperature.

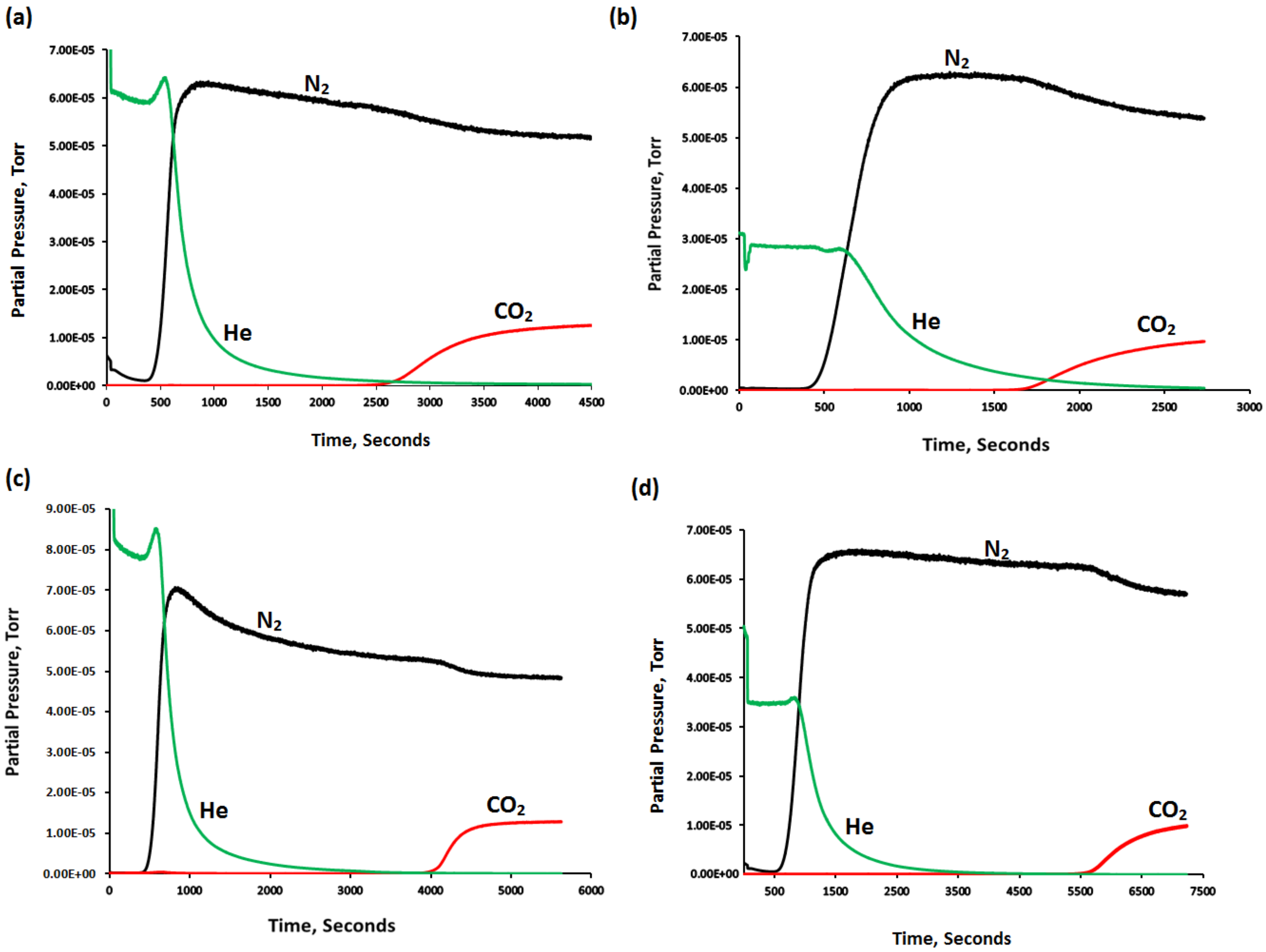

Figure S5: Column breakthrough experiments of 15:85 CO_2/N_2mixture in (a) SIFISIX-3-Zn, (b) SIFISIX-3-Cu, SIFISIX-3-Ni and SIFISIX-3-Co under dry conditions.

In situ PXRD:

The experiment was performed at Beamline 17-BM of Advanced Photon Source using monochromatic radiation (λ = 0.72768 Å). Powder samples of SIFSIX-3-Ni and SIFSIX-3-Co were loaded into an environmetal cell setup.[15] The samples were activated at 80 ˚C under 1 atm He environment until no observable change of the XRD profiles, which took less than 30 min. The samples were then cooled to room temperature, at which He was replaced with CO_2. Rietveld refinement was carried out with program GSAS.[16] In the refinement, constraints were applied to C-C, C-N, C-H bond lengths and C-N-C, N-C-H bond angles in the pyrazine group. The displacement factor (Uiso) for H was fixed to 1.2 times of that for C.

Table S2 Lattice parameters and Atomic positions of SIFSIX-3-Ni from Rietveld refinement

P 4/m m m a = 6.9942(1) Å c = 7.4941(2) Å R_{wp} = 5.4%						
Atom	Site	X	Y	Z	Occ.	U_{iso} (Å^2)
Ni	1d	½	½	½	1	0.016(1)
Si	1c	½	½	0	1	0.035(2)
F1	2h	½	½	0.7645(6)	1	0.023(1)
F2	4j	0.6665(3)	0.6665(3)	0	1	0.046(1)
N	4o	0.8016(4)	½	½	1	0.017(2)
C	16u	0.9003(1)	0.4461(6)	0.6446(3)	0.5	0.033(2)
H	16u	0.8153(10)	0.4028(11)	0.7609(5)	0.5	0.039(3)

Table S3 Lattice parameters and Atomic positions of SIFSIX-3-Ni sorbed with CO_2

P 4/m m m a = 6.9631(2) Å c = 7.5024(2) Å R_{wp} = 6.5%						
Atom	Site	X	Y	Z	Occ.	U_{iso} (Å^2)
Ni	1d	½	½	½	1	0.011(1)
Si	1c	½	½	0	1	0.033(2)
F1	2h	½	½	0.7655(7)	1	0.032(2)
F2	4j	0.6647(3)	0.6647(3)	0	1	0.051(2)
N	4o	0.8010(5)	½	½	1	0.023(2)
C	16u	0.9000(1)	0.4394(6)	0.6422(3)	0.5	0.035(3)
H	16u	0.8166(12)	0.3906(11)	0.7565(6)	0.5	0.042(3)
C of CO_2	1a	0	0	0	1	0.206(4)
O of CO_2	2g	0	0	0.1556(3)	1	0.206(4)

Table S4 Lattice parameters and Atomic positions of SIFSIX-3-Co from Rietveld refinement

P 4/m m m a = 7.1116(1) Å c = 7.5118(2) Å R_{wp} = 8.2%						
Atom	Site	X	Y	Z	Occ.	U_{iso} (Å^2)
Co	1d	½	½	½	1	0.005(1)
Si	1c	½	½	0	1	0.024(2)
F1	2h	½	½	0.7693(8)	1	0.020(2)
F2	4j	0.6681(4)	0.6681(4)	0	1	0.035(2)
N	4o	0.8024(6)	½	½	1	0.009(2)
C	16u	0.9026(1)	0.4421(6)	0.6402(4)	0.5	0.004(2)
H	16u	0.8309(14)	0.3957(11)	0.7529(7)	0.5	0.005(3)

Table S5 Lattice parameters and Atomic positions of SIFSIX-3-Co sorbed with CO_2

P 4/m m m a = 7.0769(1) Å c = 7.5212(2) Å R_{wp} = 7.3%						
Atom	Site	X	Y	Z	Occ.	U_{iso} (Å^2)
Co	1d	½	½	½	1	0.014(1)
Si	1c	½	½	0	1	0.028(2)
F1	2h	½	½	0.7651(8)	1	0.035(2)
F2	4j	0.6675(3)	0.6675(3)	0	1	0.042(2)
N	4o	0.8035(5)	½	½	1	0.015(2)
C	16u	0.9018(1)	0.4373(6)	0.6400(3)	0.5	0.013(2)
H	16u	0.8245(13)	0.3870(10)	0.7525(6)	0.5	0.016(3)
C of CO_2	1a	0	0	0	1	0.259(4)
O of CO_2	2g	0	0	0.1554(4)	1	0.259(4)

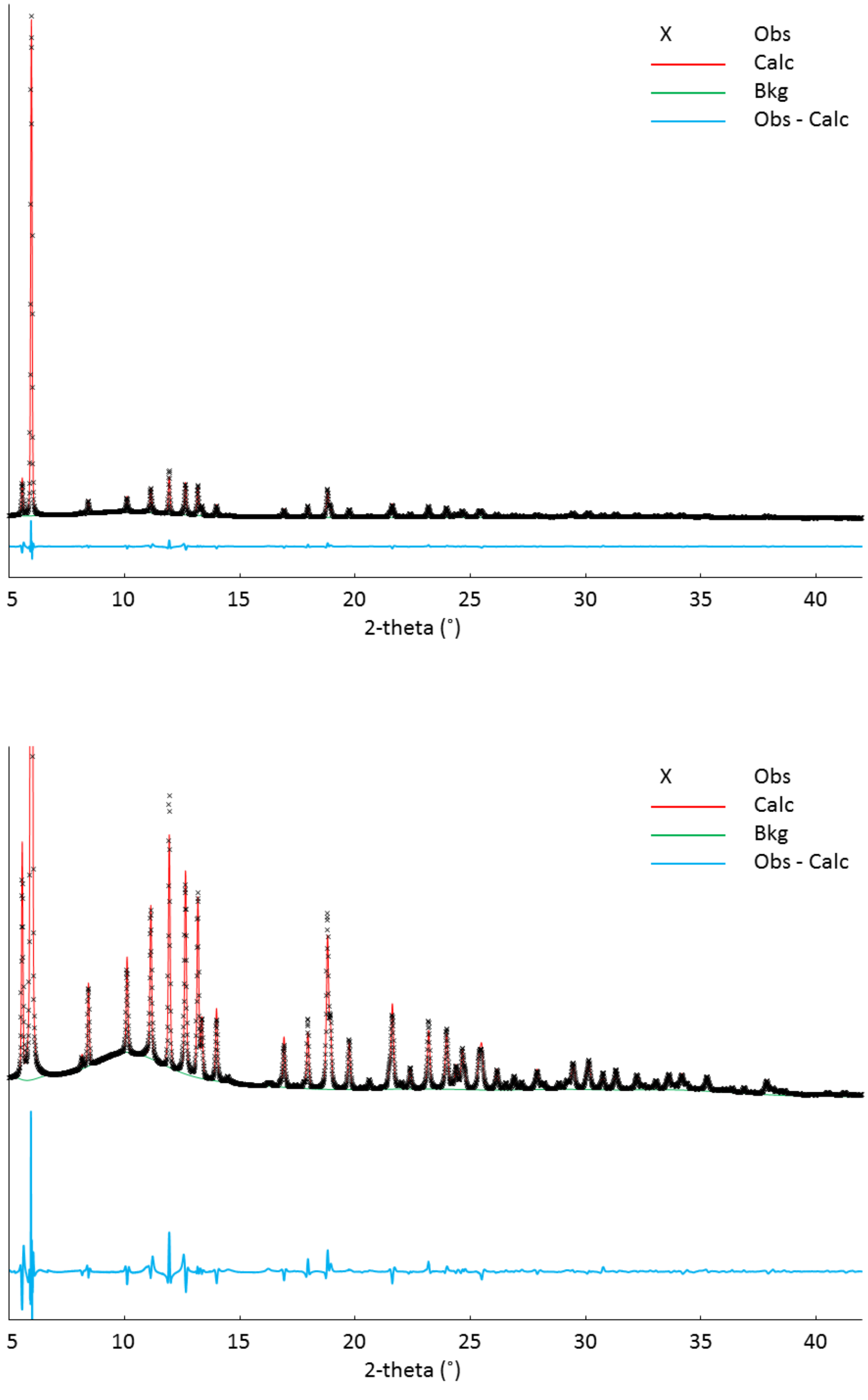

Figure S6: Rietveld fitting of the PXRD pattern of SIFSIX-3-Ni (top) and a zoomed-in graph to show fitting of the weak peaks (bottom).

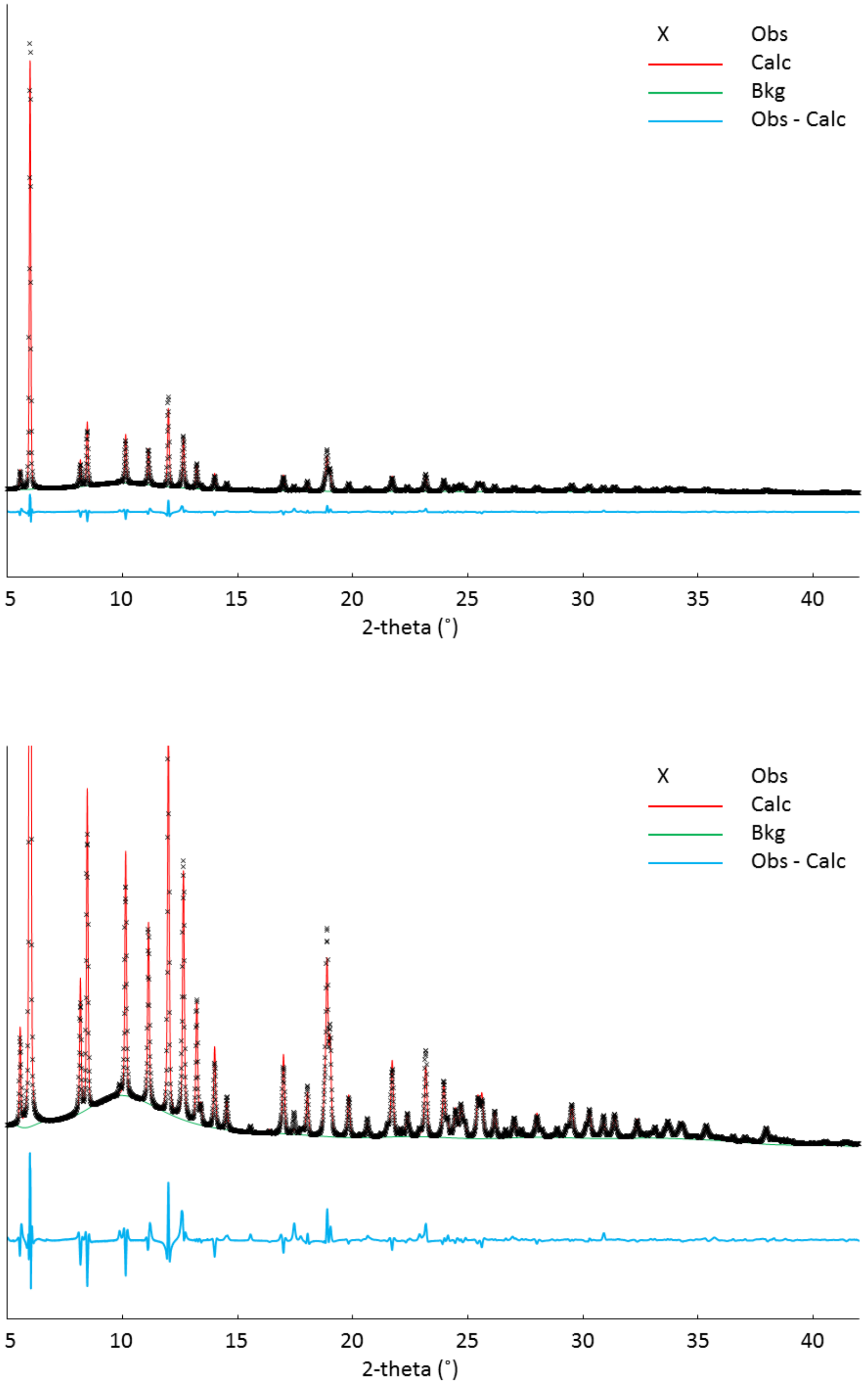

Figure S7: Rietveld fitting of the PXRD pattern of SIFSIX-3-Ni sorbed with CO_2 (top) and a zoomed-in graph to show fitting of the weak peaks (bottom).

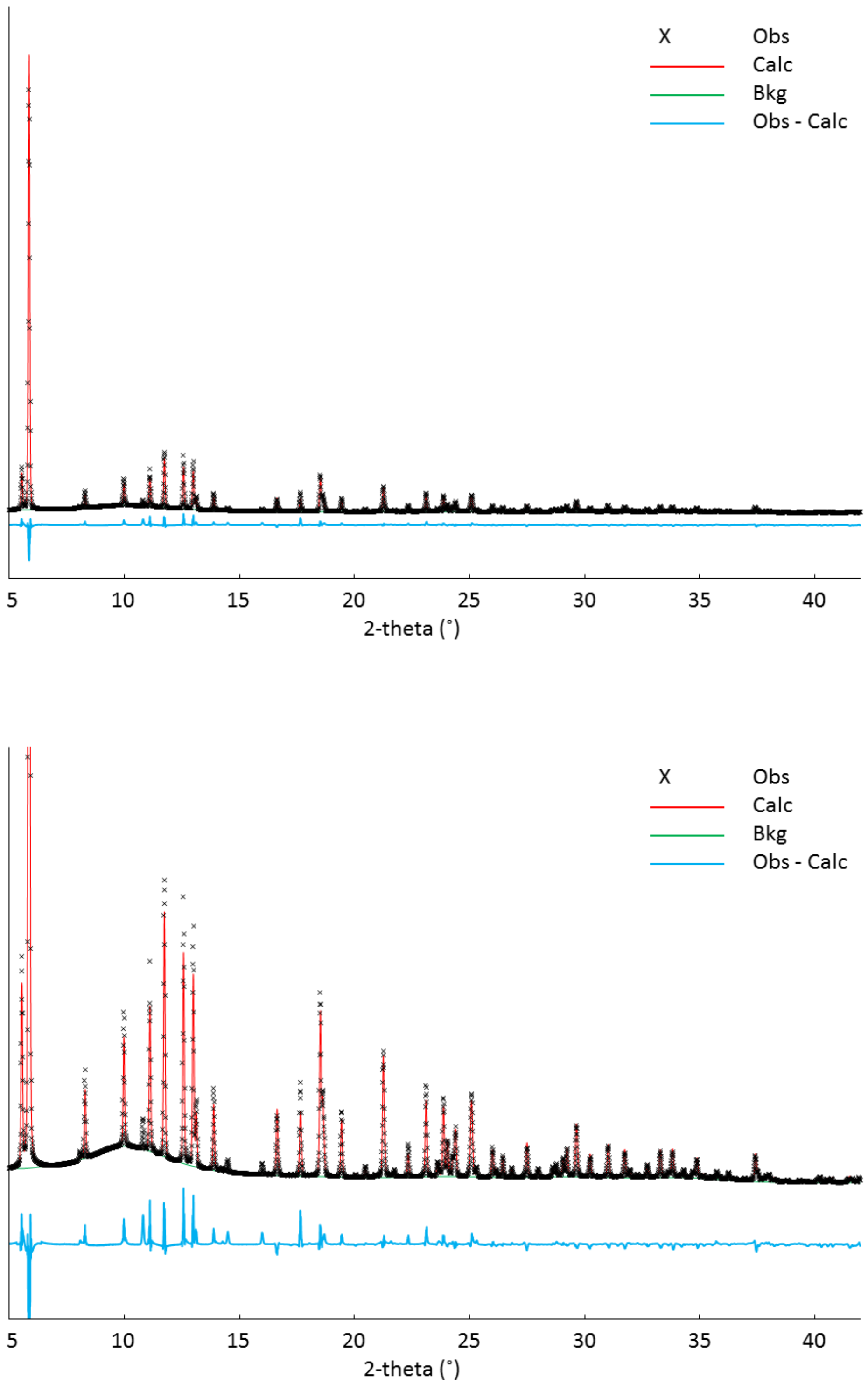

Figure S8: Rietveld fitting of the PXRD pattern of SIFSIX-3-Co (top) and a zoomed-in graph to show fitting of the weak peaks (bottom).

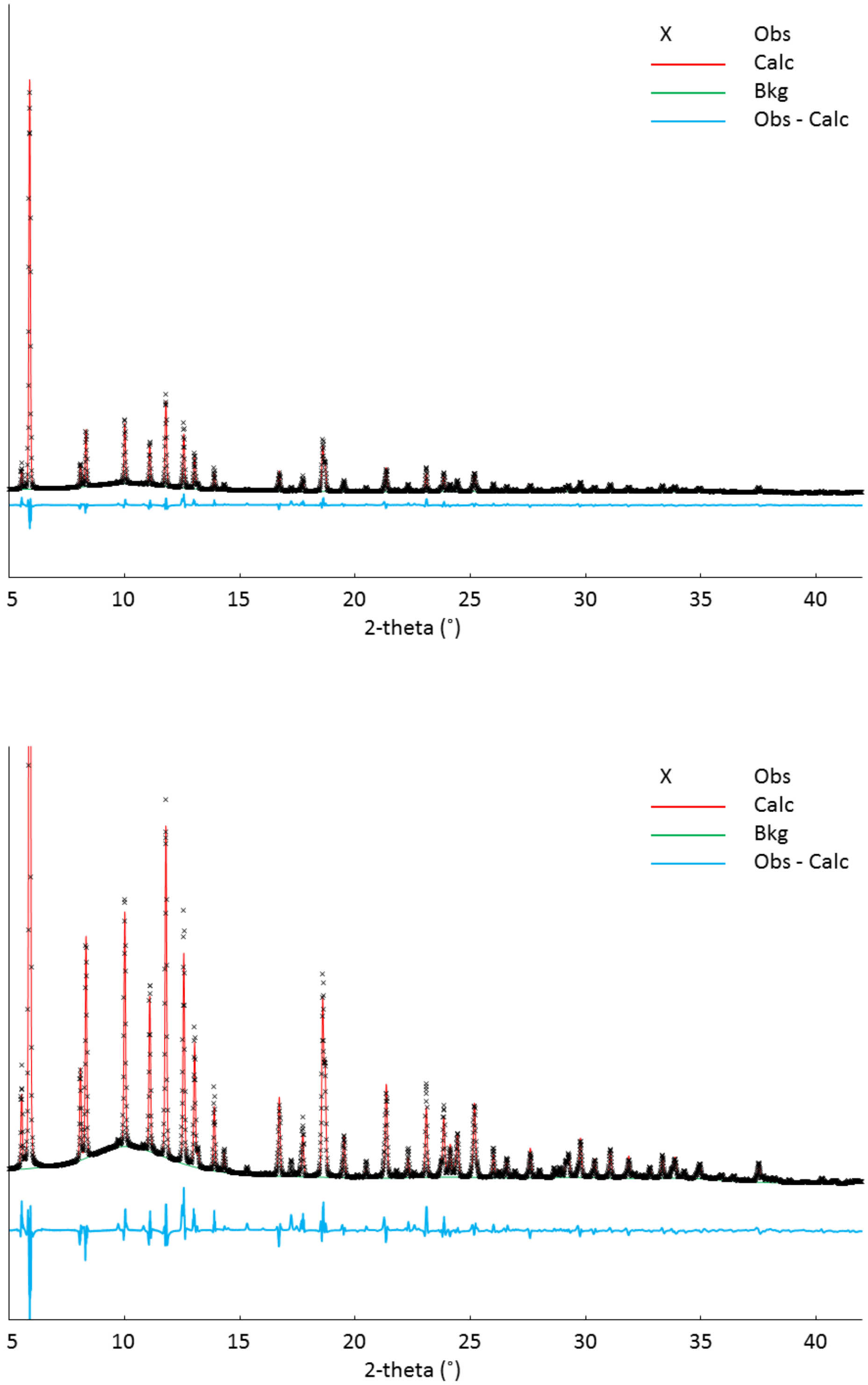

Figure S9: Rietveld fitting of the PXRD pattern of SIFSIX-3-Co sorbed with CO_2 (top) and a zoomed-in graph to show fitting of the weak peaks (bottom).

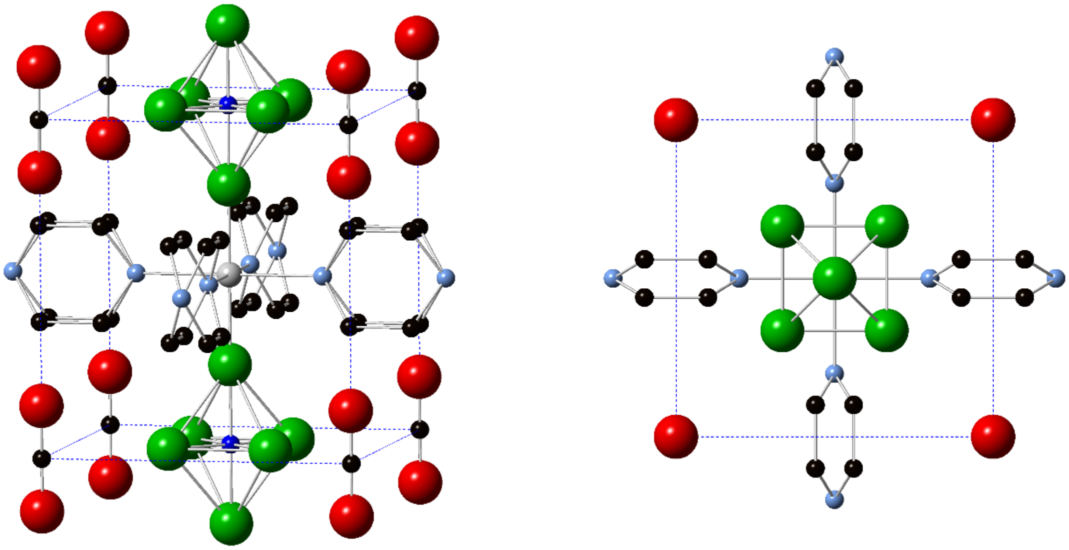

Figure S10: Side (left) and top (right) view of the crystal structure of SIFSIX-3-Ni sorbed with CO_2. Note the deviation of the pyrizane plane from the c-axis.

Modeling Details and Results

The experimental X-ray crystal structures for **SIFSIX-3-M (M = Zn, Cu, Ni, Co)**were used for the parametrizations and simulations for the respective MOMs in this work. The crystal structures for **SIFSIX-3-Zn** and **SIFSIX-3-Cu** were obtained from references 1 and 2, respectively, while the crystal structures for **SIFSIX-3-Ni** and **SIFSIX-3-Co**were established herein.The partial charges for the chemically distinct atoms (**Figure S13**) in **SIFSIX-3-M (M = Zn, Cu, Ni, Co)** were determined through electronic structure calculations on several representational gas phase fragments that were extracted from the crystal structure of the respective MOMs. This protocol was used to obtain such parameters for MOMs in previous work.[3] Model fragments for **SIFSIX-3-Co** can be found as XYZ files in the compressed folder for this manuscript. Note, fragments of similar type were also chosen for the other three members.

All calculations on each fragment were implemented using the NWChem*ab initio* software.[4] For these calculations, all C, H, N, F, and Si atoms were treated at the 6-31G* level of theory. For the many-electron metal atoms (Zn, Cu, Ni, and Co), the LANL2DZ ECP basis set[5] was used. The partial charges were determined through a least-squares fit approach[6,7] to the calculated electrostatic potential surface of each fragment. For each chemically distinct atom, the partial charges were averaged between the fragments. The averaged partial charges for each chemically distinct atom for all four MOMs can be found in **Table S6**.

Simulations of CO_2 adsorption were performed in **SIFSIX-3-M (M = Zn, Cu, Ni, and Co)** using grand canonical Monte Carlo (GCMC) methods.[8]The simulations were performed in the 3 × 3 × 3 system cells of the respective MOMs. All MOM atoms were constrained to be rigid for the simulations. For CO_2 adsorption, a five-site polarizable CO_2 potential that was developed previously was used for the simulations in this work.[9]A spherical cut-off distance corresponding to half the shortest system cell dimension length was used for the simulations. The chemical potential for $CO_2$was determined for a range of temperatures through the Peng-Robinson equation of state.[10]The total potential energy of the MOM–CO_2 system was calculated as the sum of the Lennard-Jones potential energy, the electrostatic energy as calculated by Ewald summation,[11] and the many-body polarization energy as calculated using a Thole-Applequist type model.[12] All simulations were performed using the Massively Parallel Monte Carlo (MPMC) code.[13]The simulated CO_2 adsorption isotherms for all four variants at 298 K and up to 1 atm is shown in **Figure S14**. The simulated isostericheat of adsorption (Q_{st}) values were calculated using an equation that is based on fluctuations in the particle number and the total potential energy of the system.[14]These CO_2 Q_{st} values are compared to the corresponding experimental values for all four MOMs in **Figure S15**.

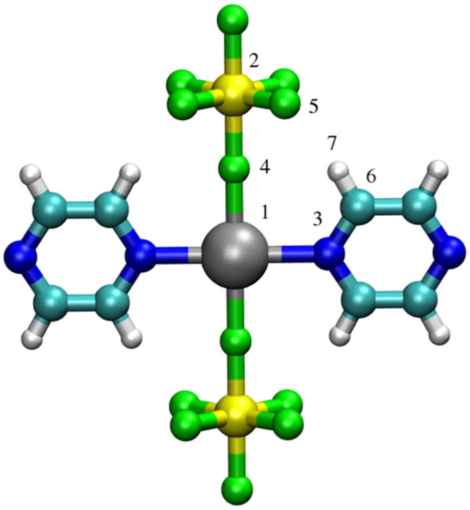

Figure S11: The numbering of the chemically distinct atoms in **SIFSIX-3-M (M = Zn, Cu, Ni, Co)** as referred to in **Table S6**. Atom colors: C = cyan, H = white, N = blue, F = green, Si = yellow, Zn/Cu/Ni/Co = silver.

Table S6: The calculated partial charges (e^-) for the chemically distinct atoms in **SIFSIX-3-M (M = Zn, Cu, Ni, Co)**. Labeling of atoms correspond to **Figure S13**.

Atom	**Label**	**SIFSIX-3-Zn**	**SIFSIX-3-Cu**	**SIFSIX-3-Ni**	**SIFSIX-3-Co**
M	1	0.97253	0.41780	0.36470	1.03850
Si	2	1.75079	1.80360	1.80690	1.90810
N	3	–0.30470	–0.06370	–0.10420	–0.33920
F	4	–0.55344	–0.64030	–0.61620	–0.65930
F	5	–0.56285	–0.59730	–0.62320	–0.64160

C	6	0.11496	0.06050	0.03780	0.12790
H	7	0.11676	0.15240	0.20850	0.15900

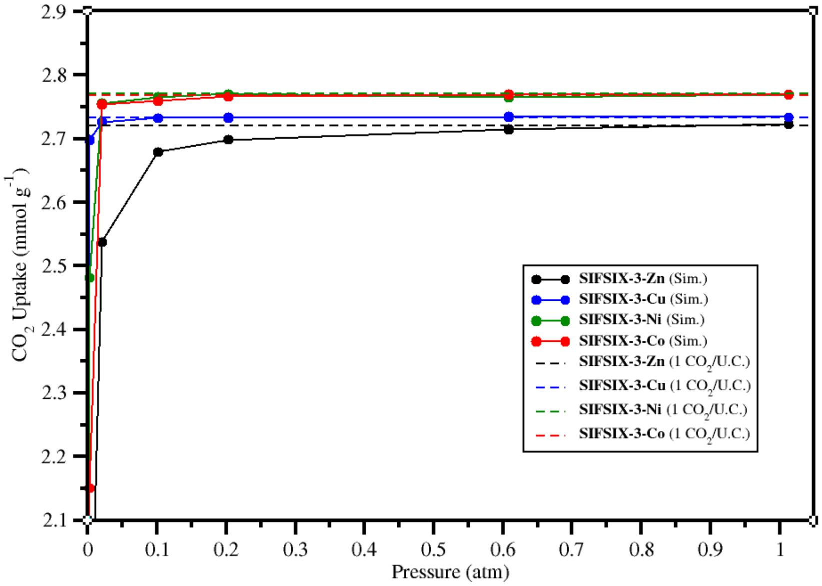

Figure S12: The simulated CO_2 adsorption isotherms in **SIFSIX-3-Zn** (black), **SIFSIX-3-Cu** (blue), **SIFSIX-3-Ni** (green), and **SIFSIX-3-Co** (red) at 298 K and pressures up to 1 atm. The dashed colored lines represent the CO_2 uptake corresponding to CO_2 saturation (1 CO_2 molecule per unit cell) for the respective MOMs.

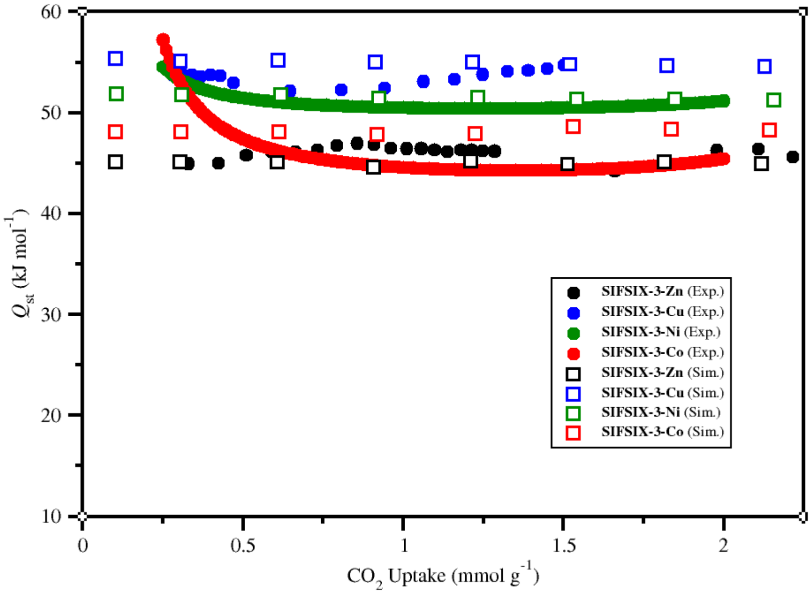

Figure S13: The experimental (circles) and simulated (squares) isosteric heat of adsorption (Q_{st}) values for CO_2 in**SIFSIX-3-Zn** (black), **SIFSIX-3-Cu** (blue), **SIFSIX-3-Ni** (green), and **SIFSIX-3-Co** (red). The experimental data for **SIFSIX-3-Zn** and **SIFSIX-3-Cu** were estimated from references 15 and 2, respectively, while those for **SIFSIX-3-Ni** and **SIFSIX-3-Co** were calculated in this work (see **Figure S6**).

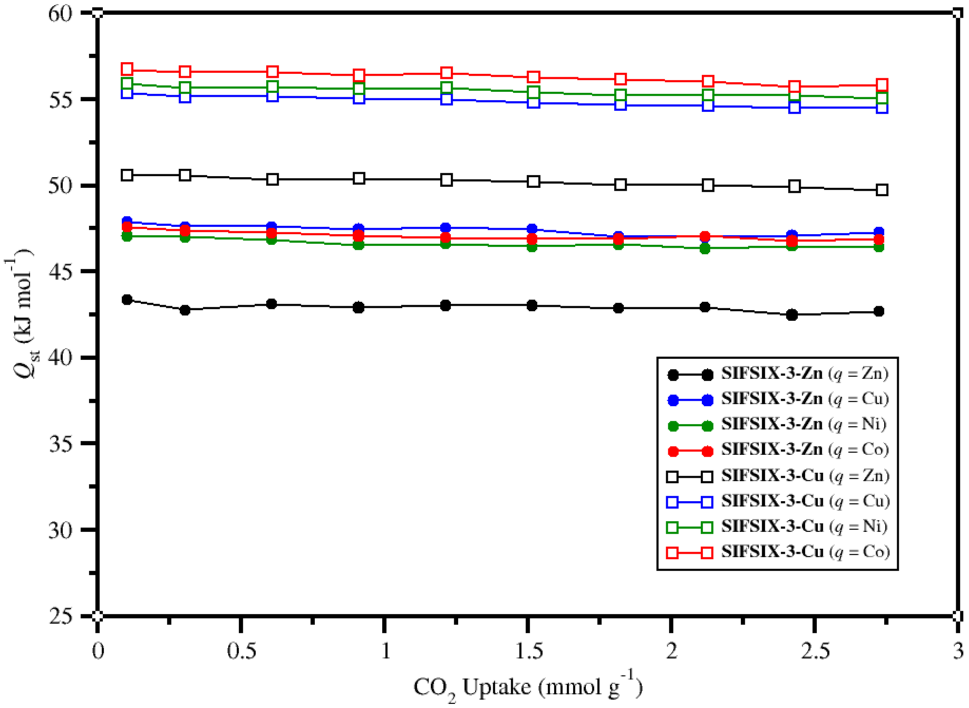

Figure S14: The simulated isosteric heat of adsorption (Q_{st}) values for CO_2in hypothetical systems of **SIFSIX-3-Zn**(circles)with electrostatic parameters derived from the **SIFSIX-3-Zn** (black), **SIFSIX-3-Cu** (blue), **SIFSIX-3-Ni** (green), and **SIFSIX-3-Co** (red) crystal structures, respectively. A similar set of $CO_2$$Q_{st}$ values in hypothetical systems of **SIFSIX-3-Cu** (squares) are also shown to illustrate the effects of the *a*/*b* lattice parameters on the MOM–CO_2 interaction strength.

References

1.) Uemura, K.; Maeda, A.; Maji, T. K.; Kanoo, P.; Kita, H. *Eur. J. Inorg. Chem.***2009**, 2329–2337.

2.) Shekhah, O.; Belmabkhout, Y.; Chen, Z.; Guillerm, V.; Cairns, A.; Adil, K.; Eddaoudi, M. *Nat. Commun.***2014**, *5*, 4228.

3.) Forrest, K. A.; Pham, T.; Hogan, A.; McLaughlin, K.; Tudor, B.; Nugent, P.; Burd, S. D.; Mullen, A.; Cioce, C. R.; Wojtas, L.; Zaworotko, M. J.; Space, B. *J. Phys. Chem. C***2013**, *117*, 17687–17698.

4.) Valiev, M.; Bylaska, E.; Govind, N.; Kowalski, K.; Straatsma, T.; Dam, H. V.; Wang, D.; Nieplocha, J.; Apra, E.; Windus, T.; de Jong, W. *Comput. Phys. Commun.* **2010**, *181*, 1477–1489.

5.) (a) Stevens, W. J.; Basch, H.; Krauss, M. *J. Chem. Phys*. **1984**, *81*, 6026–6033. (b) Hay, P. J.; Wadt, W. R. *J. Chem. Phys*. **1985**, *82*, 270–283. (c) LaJohn, L. A.; Christiansen, P. A.; Ross, R. B.; Atashroo, T.; Ermler, W. C. *J. Chem. Phys*. **1987**, *87*, 2812–2824.

6.) Chirlian, L. E.; Francl, M. M. *J. Comput. Chem*. **1987**, *8*, 894–905.

7.) Breneman, C. M.; Wiberg, K. B. *J. Comput. Chem*. **1990**, *11*, 361–373.

8.) Metropolis, N.; Rosenbluth, A. W.; Rosenbluth, M. N.; Teller, A. H.; Teller, E. *Phys. Lett. B***1953**, *21*, 1087–1092.

9.) Mullen, A. L.; Pham, T.; Forrest, K. A.; Cioce, C. R.; McLaughlin, K.; Space, B. *J. Chem. Theory Comput*. **2013**, *9*, 5421–5429.

10.) Peng, D.-Y.; Robinson, D. B. *Ind. Eng. Chem. Fundam*. **1976**, *15*, 59–64.

11.) Ewald, P. P.; *Ann. Phys*. **1921**, *369*, 253–287.

12.) (a) Applequist, J.; Carl, J. R.; Fung, K.-K. *J. Am. Chem. Soc*. **1972**, *94*, 2952–2960. (b) Thole, B. *Chem. Phys*. **1981**, *59*, 341−350. (c) Bode, K. A.; Applequist, J. *J. Phys. Chem*.**1996**, *100*, 17820–17824. (d) McLaughlin, K.; Cioce, C. R.; Pham, T.; Belof, J. L.; Space, B. *J. Chem. Phys*. **2013**, *139*, 184112.

13.) Belof, J. L.; Space, B. *Massively Parallel Monte Carlo (MPMC)*. **2012**, Available onGitHub.https://github.com/mpmccode/mpmc.

14.) Nicholson, D.; Parsonage, N. G. *Computer Simulation and the Statistical Mechanics of Adsorption*; Academic Press: London, 1982; pp. 97.

15.) Nugent, P.; Belmabkhout, Y.; Burd, S. D.; Cairns, A. J.; Luebke, R.; Forrest, K.; Pham, T.; Ma, S.; Space, B.; Wojtas, L.; Eddaoudi, M.; Zaworotko, M. J. *Nature* **2013**, *495*, 80–84.